Ocean Systems Engineering, *Vol. 5, No. 3 (2015) 221-243*
DOI: http://dx.doi.org/10.12989/ose.2015.5.3.221

Comparison of simplified model and FEM model in coupled analysis of floating wind turbine

Byoung Wan Kim*, Sa Young Hong, Hong Gun Sung and Seok Won Hong

Korea Research Institute of Ships & Ocean Engineering (KRISO), 1312-32 Yuseong-daero, Yuseong-Gu, Daejeon 34103, Korea

(Received June 3, 2015, Revised August 4, 2015, Accepted September 7, 2015)

Abstract. This paper compares simplified and finite element method (FEM) models for tower and blade in dynamic coupled analysis of floating wind turbine. A SPAR type wind turbine with catenary mooring lines is considered in numerical analysis. Floating body equation is derived using boundary element method (BEM) and convolution. Equations for mooring line, tower and blade are formulated with theories of catenary, elastic beam and aerodynamic rotating beam, respectively and FEM is applied in the formulation. By combining the equations, coupled solutions are calculated. Tower or blade may be assumed rigid or lumped body for simplicity in modeling. By comparing floating body motions, mooring line tensions and tower stresses with the simple model and original FEM model, the effect of including or neglecting elastic, rotating and aerodynamic behavior of tower and blade is discussed.

Keywords: floating wind turbine; tower; blade; coupled analysis; simplified model; FEM

1. Introduction

Offshore wind turbine is one of hot topics in ocean engineering field and has been discussed by many previous studies (Shim and Kim 2008, Jonkman *et al.* 2009, 2010, Bae *et al*. 2011, 2012, 2013, 2014). Since wind turbine has blade system and its supporting tower, the behavior in waves may be different from conventional floating bodies. For example, elastic effect of tower and elastic, aerodynamic & rotating effect of blade could affect floating body motions or mooring line tensions. Therefore, numerical simulation requires more rigorous model in order to include such distributed properties of tower and blade. FEM is one of the models. Rigorous model for tower and blade will provide more correct results but it requires more efforts in modeling. If simplified modeling is allowed, tower or blade could be assumed one point rigid or lumped mass. It can reduce modeling time but gives results in a roughly manner because the mass distribution, elasticity and aerodynamics are not considered.

The objective of this study is to compare simplified and FEM models for tower and blade in dynamic coupled analysis of floating wind turbine. To do this, a SPAR type wind turbine studied by Jonkman *et al*. (2009, 2010) is analyzed. Hydrodynamic mass, damping and force of floating body is calculated by BEM (Choi *et al*. 2000, Hong *et al*. 2005) and the results is converted to time

*Corresponding author, Dr., E-mail: kimbw@kriso.re.kr

http://www.techno-press.org/?journal=ose&subpage=7 ISSN: 2093-6702 (Print), 2093-677X (Online)

domain with convolution method (Cummins 1962). Catenary formulation for mooring line dynamics were studied by many previous studies (Hong and Hong 1997, Kim *et al*. 1999, Garrett 2005, Shim and Kim 2008, Kim *et al.* 2010, Kim *et al*. 2013). Among them, this study applied FEM by Kim *et al*. (2010, 2013). Tower dynamics are formulated with elastic beam model using FEM. In simplified model, it is modeled as a rigid body. Blade behaviors are simulated with elastic rotating beam model using FEM and aerodynamic wind forces are considered. In simplified model, the blade is assumed a lumped body. Coupled equation is formulated by combining equations of floating body, mooring line, tower and blade with considering compatibility of forces and motions at connections such as fairleads and tower base. Time marching is done using Hamming method (Hamming 1959) and generalized-α Newmark method (Chung and Hulbert 1993). In modeling of tower and blade, four comparison cases such as rigid tower & lumped blade, rigid tower & FEM blade, FEM tower & lumped blade and FEM tower & FEM blade are considered. By analyzing surge, heave, pitch, mooring line tensions and tower base stresses for the four cases, the simplified model and FEM model are compared and their differences are discussed.

2. Equation of motion for floating wind turbine

Time domain equation for floating body part of wind turbine can be expressed by

$$[M_B + M_{add}(\infty)]\{\ddot{x}\} + \int_0^t [R(t-\tau)]\{\dot{x}(\tau)\}d\tau + [K_B]\{x\} = \{f_B\} + \{f_c\} \tag{1}$$

where $[M_B]$ and $[K_B]$ are mass and hydrostatic matrix of floating body. $\{x\}$ is vector of floating body motions. $[M_{add}(\infty)]$ is added mass matrix at infinite frequency and R is retardation function. $\{f_B\}$ is vector of forces acting at floating body such as wave and drift. This study applied convolution method (Hamming 1959) to derive (1). Convolution method converts frequency domain equation to time domain equation. In this study, higher order BEM (Choi *et al.* 2000, Hong *et al.* 2005) is used to get frequency domain equation. $\{f_c\}$ is body forces transmitted from the forces at connections between floating body and mooring, tower & blade. Fairleads and tower base are those connections. These connection forces come from the results of equation for mooring lines, tower and blades.

Formulation of mooring lines is already studied by many researches. Hong and Hong (1997) and Kim *et al*. (2010) analyzed mooring lines using catenary theory including axial stiffness effect. More advanced forms were presented by some researchers (Kim *et al*. 1999, Garrett 2005, Shim and Kim 2008). They considered bending stiffness as well as axial stiffness. More general formulation was done based on FEM (Kim *et al*. 2013). It can include axial, bending and torsion effects. Lines with more complicated geometry such as net or web are also applicable because it is based on FEM formulation. This paper followed FEM by Kim *et al*. (2013) and the details are omitted in this paper. This paper focuses on formulation of blade and tower. Elastic rotating beam model is applied in FEM formulation of blade. The configuration is shown in Fig. 1. The total energy due to axial deformation, bending, torsion, kinetic movement, section forces will be

$$\pi = \frac{1}{2}\int_0^l EA\bar{u}_x'^2 d\bar{x} + \frac{1}{2}\int_0^l EI_y \bar{u}_z''^2 d\bar{x} + \frac{1}{2}\int_0^l EI_z \bar{u}_y''^2 d\bar{x} + \frac{1}{2}\int_0^l GJ\bar{\theta}_x'^2 d\bar{x}$$
$$- \frac{1}{2}\int_0^l m(\dot{u}_x{}^2 + \dot{u}_y{}^2 + \dot{u}_z{}^2) d\bar{x} - \frac{1}{2}\int_0^l I_m \dot{\bar{\theta}}_x{}^2 d\bar{x} - \{\bar{u}_e\}^T \{\bar{f}_e\} \tag{2}$$

where EA is axial stiffness of an element, EI_y is bending stiffness about $\bar{y}$ axis, EI_z is bending stiffness about $\bar{z}$ axis, GJ is torsion stiffness, m is mass per unit length, I_m rotational mass per unit length. $\{\bar{u}_e\}$ and $\{\bar{f}_e\}$ are nodal displacements and section forces in local coordinate.

$$\{\bar{u}_e\} = [\bar{u}_{x1}\ \bar{u}_{y1}\ \bar{u}_{z1}\ \bar{\theta}_{x1}\ \bar{\theta}_{y1}\ \bar{\theta}_{z1}\ \bar{u}_{x2}\ \bar{u}_{y2}\ \bar{u}_{z2}\ \bar{\theta}_{x2}\ \bar{\theta}_{y2}\ \bar{\theta}_{z2}]^T \tag{3}$$

$$\{\bar{f}_e\} = [\bar{f}_{x1}\ \bar{f}_{y1}\ \bar{f}_{z1}\ \bar{M}_{x1}\ \bar{M}_{y1}\ \bar{M}_{z1}\ \bar{f}_{x2}\ \bar{f}_{y2}\ \bar{f}_{z2}\ \bar{M}_{x2}\ \bar{M}_{y2}\ \bar{M}_{z2}]^T \tag{4}$$

In (2), internal displacements in element can be interpolated with nodal displacements as

$$\begin{aligned}
\bar{u}_x &= [N_1\ 0\ 0\ 0\ 0\ 0\ N_2\ 0\ 0\ 0\ 0\ 0]\{\bar{u}_e\} \\
\bar{u}_y &= [0\ H_1\ 0\ 0\ 0\ H_2\ 0\ H_3\ 0\ 0\ 0\ H_4]\{\bar{u}_e\} \\
\bar{u}_z &= [0\ 0\ H_1\ 0\ -H_2\ 0\ 0\ 0\ H_3\ 0\ -H_4\ 0]\{\bar{u}_e\} \\
\bar{\theta}_x &= [0\ 0\ 0\ N_1\ 0\ 0\ 0\ 0\ 0\ N_2\ 0\ 0]\{\bar{u}_e\}
\end{aligned}$$

where

$$N_1 = 1 - \bar{x}/l\,,\ \ N_2 = \bar{x}/l \tag{5}$$

are Lagrange interpolation functions and

$$\begin{aligned}
H_1 &= 1 + 2(\bar{x}/l)^3 - 3(\bar{x}/l)^2\,,\ \ H_2 = x\{(\bar{x}/l) - 1\}^2 \\
H_3 &= 3(\bar{x}/l)^2 - 2(\bar{x}/l)^3\,,\ \ H_4 = x\{(\bar{x}/l)^2 - (\bar{x}/l)\}^2
\end{aligned} \tag{6}$$

are Hermite interpolation functions. In bending formulation, Hermite interpolation is generally applied because bending solution is higher order. Inserting (5) and (6) to (2) and minimizing it

$$\frac{\partial \pi}{\partial\{\bar{u}_e\}} - \frac{d}{dt}\frac{\partial \pi}{\partial\{\dot{\bar{u}}_e\}} = 0 \tag{7}$$

will lead to the following element equation of motion in local coordinate.

$$[M_e]\{\ddot{\bar{u}}_e\} + [K_e]\{\bar{u}_e\} = \{\bar{f}_{ce}\} + \{\bar{f}_e\} \tag{8}$$

where

$$[M_e]=\begin{bmatrix} 0 & 0 & 0 & 0 & 0 & 0 & 0 & 0 & 0 & 0 & 0 & 0 \\ & \frac{156ml}{420} & 0 & 0 & 0 & \frac{22ml^2}{420} & 0 & \frac{54ml}{420} & 0 & 0 & 0 & -\frac{13ml^2}{420} \\ & & 0 & 0 & 0 & 0 & 0 & 0 & 0 & 0 & 0 & 0 \\ & & & \frac{I_m l}{3} & 0 & 0 & 0 & 0 & 0 & \frac{I_m l}{6} & 0 & 0 \\ & & & & 0 & 0 & 0 & 0 & 0 & 0 & 0 & 0 \\ & & & & & \frac{4ml^3}{420} & 0 & \frac{13ml^2}{420} & 0 & 0 & 0 & -\frac{3ml^3}{420} \\ & & & & & & 0 & 0 & 0 & 0 & 0 & 0 \\ & & & & & & & \frac{156ml}{420} & 0 & 0 & 0 & -\frac{22ml^2}{420} \\ & & & & & & & & 0 & 0 & 0 & 0 \\ & & & & & & & & & \frac{I_m l}{3} & 0 & 0 \\ & & & & & & & & & & 0 & 0 \\ & & & & & & & & & & & \frac{4ml^3}{420} \end{bmatrix} \tag{9}$$

$$[K_e]=\begin{bmatrix} \frac{EA}{l} & 0 & 0 & 0 & 0 & 0 & -\frac{EA}{l} & 0 & 0 & 0 & 0 & 0 \\ & \frac{12EI_z}{l^3} & 0 & 0 & 0 & \frac{6EI_z}{l^2} & 0 & -\frac{12EI_z}{l^3} & 0 & 0 & 0 & \frac{6EI_z}{l^2} \\ & & \frac{12EI_y}{l^3} & 0 & -\frac{6EI_y}{l^2} & 0 & 0 & 0 & -\frac{12EI_y}{l^3} & 0 & -\frac{6EI_y}{{}_z l^2} & 0 \\ & & & \frac{GJ}{l} & 0 & 0 & 0 & 0 & 0 & -\frac{GJ}{l} & 0 & 0 \\ & & & & \frac{4EI_y}{l} & 0 & 0 & 0 & \frac{6EI_y}{l^2} & 0 & \frac{2EI_y}{l} & 0 \\ & & & & & \frac{4EI_z}{l} & 0 & -\frac{6EI_z}{l^2} & 0 & 0 & 0 & \frac{2EI_z}{l} \\ & & & & & & \frac{EA}{l} & 0 & 0 & 0 & 0 & 0 \\ & & & & & & & \frac{12EI_z}{l^3} & 0 & 0 & 0 & -\frac{6EI_z}{l^2} \\ & & & & & & & & \frac{12EI_y}{l^3} & 0 & \frac{6EI_y}{l^2} & 0 \\ & & & & & & & & & \frac{GJ}{l} & 0 & 0 \\ & & & & & & & & & & \frac{4EI_y}{l} & 0 \\ & & & & & & & & & & & \frac{4EI_z}{l} \end{bmatrix}$$

$$-m\omega^2\begin{bmatrix} \frac{l}{3} & 0 & 0 & 0 & 0 & 0 & \frac{l}{6} & 0 & 0 & 0 & 0 & 0 \\ & 0 & 0 & 0 & 0 & 0 & 0 & 0 & 0 & 0 & 0 & 0 \\ & & \frac{156l}{420} & 0 & -\frac{22l^2}{420} & 0 & 0 & 0 & \frac{54l}{420} & 0 & \frac{13l^2}{420} & 0 \\ & & & 0 & 0 & 0 & 0 & 0 & 0 & 0 & 0 & 0 \\ & & & & \frac{4l^3}{420}0 & 0 & 0 & 0 & -\frac{13l^2}{420} & 0 & -\frac{3l^3}{420} & 0 \\ & & & & & 0 & 0 & 0 & 0 & 0 & 0 & 0 \\ & & & & & & \frac{l}{3} & 0 & 0 & 0 & 0 & 0 \\ & & & & & & & 0 & 0 & 0 & 0 & 0 \\ & & & & & & & & \frac{156l}{420} & 0 & \frac{22l^2}{420} & 0 \\ & & & & & & & & & 0 & 0 & 0 \\ & & & & & & & & & & \frac{4l^3}{420} & 0 \\ & & & & & & & & & & & 0 \end{bmatrix} \tag{10}$$

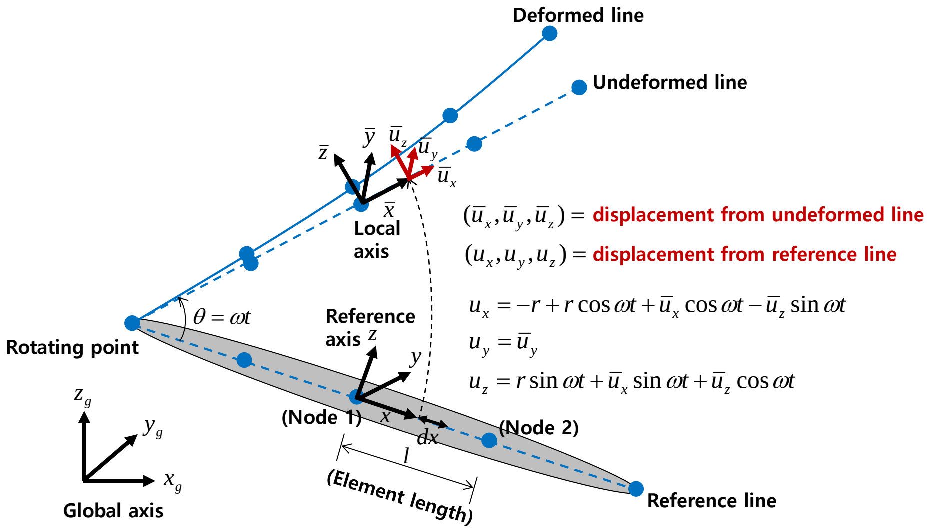

Fig. 1 Conceptual figure of FEM model of elastic rotating beam for blade

are symmetric mass and stiffness matrix of element and

$$\{\bar{f}_{ce}\} = m\omega^2 l[(r_1/3 + r_2/6)\ 0\ 0\ 0\ 0\ 0\ (r_1/6 + r_2/3)\ 0\ 0\ 0\ 0\ 0]^T \tag{11}$$

is force vector due to centrifuge. ω is rotation speed of blade. r_1 and r_2 are rotation radius at nodes 1 and 2. Displacements and forces between local and global axes satisfy the following coordinate transform.

$$\{\bar{u}_e\} = [\bar{T}][T]\{u_{ge}\} + \{\bar{s}\} \tag{12}$$

$$\{f_{ge}\} = [T]^T([\bar{T}]^T + [\tilde{T}])\{\bar{f}_e\} \tag{13}$$

where

$$[\bar{T}] = \left[\begin{array}{ccc:ccc:ccc:ccc}
\cos\omega t & 0 & \sin\omega t & & & & & & & & & \\
0 & 1 & 0 & & & & & & & & & \\
-\sin\omega t & 0 & \cos\omega t & & & & & & & & & \\ \hdashline
 & & & \cos\omega t & 0 & \sin\omega t & & & & & & \\
 & & & 0 & 1 & 0 & & & & & & \\
 & & & -\sin\omega t & 0 & \cos\omega t & & & & & & \\ \hdashline
 & & & & & & \cos\omega t & 0 & \sin\omega t & & & \\
 & & & & & & 0 & 1 & 0 & & & \\
 & & & & & & -\sin\omega t & 0 & \cos\omega t & & & \\ \hdashline
 & & & & & & & & & \cos\omega t & 0 & \sin\omega t \\
 & & & & & & & & & 0 & 1 & 0 \\
 & & & & & & & & & -\sin\omega t & 0 & \cos\omega t
\end{array}\right] \tag{14}$$

$$[\tilde{T}]=\left[\begin{array}{ccc:ccc:ccc:ccc}
 & & & & & & & & & & & \\
 & & & & & & & & & & & \\
 & & & & & & & & & & & \\ \hdashline
0 & -r_1\sin\omega t & 0 & & & & & & & & & \\
r_1\sin\omega t & 0 & r_1\cos\omega t-r_1 & & & & & & & & & \\
0 & r_1\cos\omega t-r_1 & 0 & & & & & & & & & \\ \hdashline
 & & & & & & & & & & & \\
 & & & & & & & & & & & \\
 & & & & & & & & & & & \\ \hdashline
 & & & & & & 0 & -r_2\sin\omega t & 0 & & & \\
 & & & & & & r_2\sin\omega t & 0 & r_2\cos\omega t-r_2 & & & \\
 & & & & & & 0 & r_2\cos\omega t-r_2 & 0 & & &
\end{array}\right] \tag{15}$$

$$\{\bar{s}\}=[(r_1\cos\omega t-r_1)\ 0\ -r_1\sin\omega t\ 0\ \omega t\ 0\ (r_2\cos\omega t-r_2)\ 0\ -r_2\sin\omega t\ 0\ \omega t\ 0]^T \tag{16}$$

are transform matrix between local and reference axes, $[T]$ is transform matrix between reference and global axes and

$$\{u_{ge}\}=[u_{x1g}\ u_{y1g}\ u_{z1g}\ \theta_{x1g}\ \theta_{y1g}\ \theta_{z1g}\ u_{x2g}\ u_{y2g}\ u_{z2g}\ \theta_{x2g}\ \theta_{y2g}\ \theta_{z2g}]^T \tag{17}$$

$$\{\bar{f}_e\}=[\bar{f}_{x1}\ \bar{f}_{y1}\ \bar{f}_{z1}\ \overline{M}_{x1}\ \overline{M}_{y1}\ \overline{M}_{z1}\ \bar{f}_{x2}\ \bar{f}_{y2}\ \bar{f}_{z2}\ \overline{M}_{x2}\ \overline{M}_{y2}\ \overline{M}_{z2}]^T \tag{18}$$

are nodal displacements and section forces in global coordinate. (14)~(16) can be derived using geometric relation between local and reference axes. $[T]$ can be derived in many ways and the result is shown in many engineering texts. Premultiplying (8) by $[T]^T([\overline{T}]^T+[\tilde{T}])$ and using the coordinate transform will lead to the element equation in global coordinate.

$$[M_{ge}]\{\ddot{u}_{ge}\}+[K_{ge}]\{u_{ge}\}=\{f_{gce}\}+\{f_{ge}\} \tag{19}$$

where

$$[M_{ge}]=[T]^T[\overline{T}]^T[M_e][\overline{T}][T] \tag{20}$$

$$[K_{ge}]=[T]^T[\overline{T}]^T[K_e][\overline{T}][T] \tag{21}$$

are mass and stiffness matrix of element in global coordinate and

$$\begin{aligned}\{f_{gce}\}=[T]^T([\overline{T}]^T+[\tilde{T}])(\{\bar{f}_{ce}\}-[M_e][\ddot{\overline{T}}][T]\{u_{ge}\}-2[M_e][\dot{\overline{T}}][T]\{\dot{u}_{ge}\}-[M_e]\{\ddot{\bar{s}}\}-[K_e]\{\bar{s}\})\\ -[T]^T[\tilde{T}][M_e][\overline{T}][T]\{\ddot{u}_{ge}\}-[T]^T[\tilde{T}][K_e][\overline{T}][T]\{u_{ge}\}\end{aligned} \tag{22}$$

is vector of centrifuge force in global coordinate and equivalent force due transform. Element by element combination of (22), introduction of structural damping and application of compatibility for section forces and external nodal forces will derive the equation of motion for total system

$$[M]\{\ddot{u}\}+[C]\{\dot{u}\}+[K]\{u\}=\{f\} \quad \text{with BC : } u=u_c \text{ at connections} \tag{23}$$

where $[M]$, $[K]$, $\{u\}$ and $\{f\}$ are mass matrix, stiffness matrix, displacement vector and force vector for total system. $[C]$ is structural damping matrix such as Rayleigh damping. In this study, structural damping is ignored because aerodynamic and hydrodynamic damping is already included. For example, aerodynamic damping effect is included in Morison Eq. (24). Similarly, hydrodynamic damping is also included in mooring lines with Morison form and it is discussed in the previous study by Kim *et al.* (2013). u_c is displacement at connections transmitted from floating body center. It comes from (1). Aerodynamic forces due to wind are calculated in Morison form

$$\vec{f}_{aero} = \frac{1}{2} C_D \rho |\vec{v}_r| \vec{v}_r D \Delta s \tag{24}$$

where C_D is drag coefficient, ρ is air density, D is chord, Δs is element length and

$$\vec{v}_r = (\vec{v}_w - \vec{v}_{sn}) - ((\vec{v}_w - \vec{v}_{sn}) \cdot \vec{t})\vec{t} \tag{25}$$

$$\vec{v}_{sn} = \vec{v}_s - (\vec{v}_s \cdot \vec{n})\vec{n} \tag{26}$$

are relative wind velocity and blade velocity in wind direction. $\vec{v}_w$ is wind velocity, $\vec{v}_s$ is blade velocity, $\vec{t}$ is unit radial vector and $\vec{n} = \vec{t} \times \vec{v}_w / |\vec{v}_w|$ is unit normal vector. Eq. (24) is calculated at each element and the results are added to force term of (23).

Tower can be also modeled with elastic beams like blades. The only difference is that tower does not rotate. So, the formulation can be obtained by inserting $\omega = 0$ to all system matrices and the results are added to mass and stiffness terms of (23). As already commented, mooring equation is obtained by previous studies. Mass and stiffness matrix of mooring lines are added to mass and stiffness term of (23). Morison forces acting at mooring lines are added to force terms of (23). Detailed formulation can be found in the references (Kim *et al.* 2010, Kim *et al*. 2013).

By solving (1) with numerical method such as Hamming method (Hamming 1959), displacements at connections are obtained. With this boundary conditions, (23) is solved. Then, connection forces are obtained and they go to (1). Generalized-α Newmark method (Chung and Hulbert 1993) is employed in solving (23). This process is iterated until the solution converges. In this way, coupled solution for floating body, mooring lines, tower and blade is obtained.

3. Numerical analysis and discussions

A SPAR type wind turbine studied in previous researches (Jonkman *et al.* 2009, Jonkman 2010, Jonkman and Musial 2010) is analyzed in numerical example. The sample turbine has three catenary mooring lines, a tower and three blades. Fig. 2 and Table 1 summarize geometry and particulars of the example wind turbine. Tower is modeled with elastic beam elements in FEM and its distributed structural properties are assigned as Table 2. In simple model, it is assumed a rigid mass and the lumped mass property is merged to floating body. Blades are modeled with elastic rotating beam elements in FEM and distributed aerodynamic forces due to wind are calculated. Structural and aerodynamic properties are summarized in Table 3. In simplified model, the blade is considered as a lumped mass and the value is merge to floating body data. Wind force is also simplified as a point load acting at rotation center. Wind and irregular waves are considered as environmental forces. Wind speed is assumed 25 m/s. The rotation speed of rotor is 12.1 rpm. Sea states 5 and 8 are considered in irregular waves. Wave heading is 180 deg. Environments are summarized in Table 4. In order to compare simplified and FEM models for tower and blade, four comparison cases as Table 5 are considered in numerical analyses. Case 1 uses simplified model for both tower and blade. This is the simplest case. Case 2 uses rigid body model for tower and FEM for blade. Case 3 uses FEM for tower and lumped body model for blade. Case 4 uses FEM for both tower and blade. So, case 4 is the most rigorous model. Surge, heave, pitch, tower base stress and mooring line tensions are calculated and the results of cases 1, 2 and 3 are compared with those of the most rigorous model (case 4).

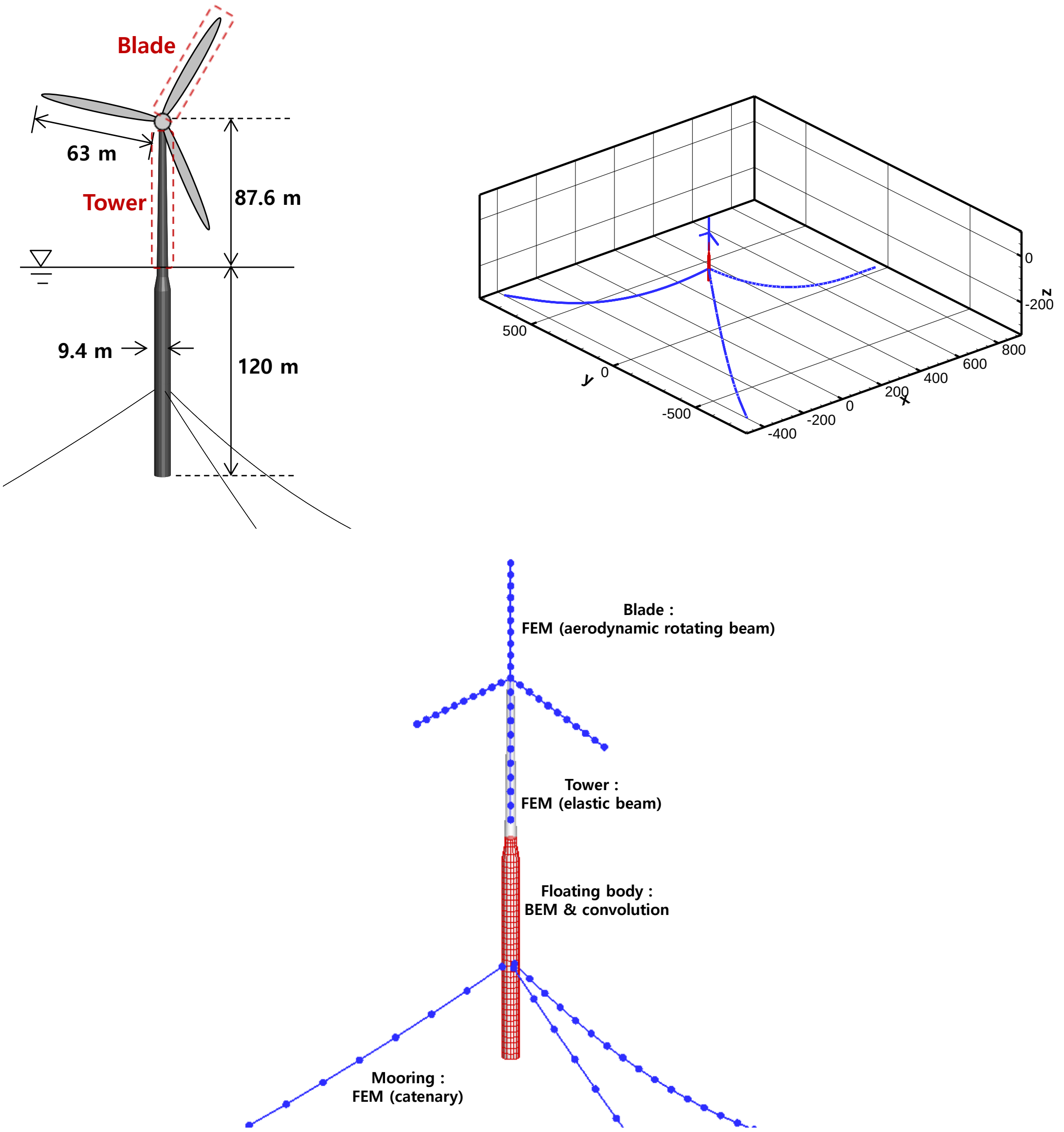

Fig. 2 Geometry of example wind turbine and its numerical model

Table 1 Main particulars of example wind turbine

Floating body	Height		207.6 m
	Draft		120 m
	Water depth		320 m
	Mass	Platform	7,466.330 ton
		Tower	249.718 ton
		Rotor	Blade(17.74 ton)×3+Hub(56.78 ton)=110 ton
		Nacelle	240 ton
		Total	8,066.048 ton
Mooring lines	No of lines		3
	Length		902.2 m
	EA		384,243,000 N
	Weight		698.094 N/m
	D		0.09 m

Table 2 Structural property of tower

Elevation (m)	D (m)	Mass (kg/m)	EA (N)	EI_y=EI_z (N-m^2)	GJ (N-m^2)
10.00	6.261	4667.00	1.153E+11	6.039E+11	4.647E+11
17.76	6.022	4345.28	1.074E+11	5.176E+11	3.983E+11
25.52	5.783	4034.76	9.968E+10	4.409E+11	3.393E+11
33.28	5.544	3735.44	9.229E+10	3.730E+11	2.870E+11
41.04	5.305	3447.32	8.517E+10	3.132E+11	2.410E+11
48.80	5.065	3170.40	7.833E+10	2.609E+11	2.008E+11
56.56	4.826	2904.69	7.176E+10	2.154E+11	1.657E+11
64.32	4.587	2650.18	6.548E+10	1.760E+11	1.355E+11
72.08	4.348	2406.88	5.946E+10	1.423E+11	1.095E+11
79.84	4.109	2174.77	5.373E+10	1.136E+11	8.744E+10
87.60	3.870	1953.87	4.827E+10	8.949E+10	6.886E+10

Table 3 Aerodynamic and structural property of blade

Radius (m)	Chord (m)	C_D	Mass (kg/m)	EA (N)	EI_y (N-m^2)	EI_z (N-m^2)	GJ (N-m^2)
3.15	3.57434	5.00000E-01	7.58597E+02	1.04645E+10	1.85389E+10	1.95312E+10	5.23467E+09
9.45	4.29447	2.39301E-01	3.86706E+02	4.14959E+09	5.11713E+09	7.17912E+09	1.26128E+09
15.75	4.64968	9.44634E-03	3.52655E+02	3.14095E+09	2.55994E+09	5.04394E+09	3.34691E+08
22.05	4.35095	9.04146E-03	3.28602E+02	2.32062E+09	1.78633E+09	4.20053E+09	2.23908E+08
28.35	3.99437	6.50000E-03	2.92259E+02	1.56760E+09	1.02874E+09	3.34702E+09	1.36511E+08
34.65	3.60400	6.03171E-03	2.47725E+02	9.88302E+08	4.74955E+08	2.44997E+09	6.35610E+07
40.95	3.22600	5.63902E-03	1.87237E+02	5.80324E+08	1.99411E+08	1.42114E+09	3.06425E+07
47.25	2.84800	5.20000E-03	1.42417E+02	3.94708E+08	9.45655E+07	8.47838E+08	1.67885E+07
53.55	2.47000	5.20000E-03	9.94126E+01	2.14033E+08	5.03477E+07	4.59619E+08	8.13575E+06
59.85	1.85417	5.20000E-03	5.83122E+01	6.02570E+07	1.85410E+07	1.52531E+08	4.06600E+06

Table 4 Wind and wave conditions

Wind speed	25 m/s		
Rotor speed	12.1 rpm		
Irregular waves	Sea state	Significant height	Modal period
	5	4.00 m	10 s
	8	15.24 m	17 s

Table 5 Analysis cases for comparison

Comparison cases	Numerical model for tower and blade	
	Tower	Blade
1	Rigid body	Lumped body
2	Rigid body	FEM (aerodynamic rotating beam)
3	FEM (elastic beam)	Lumped body
4	FEM (elastic beam)	FEM (aerodynamic rotating beam)

Analyses results are summarized in Figs. 3-12 and Table 6 and 7. Fig. 3 compares surge motion of the example wind turbine in sea state 5. Four cases show general agreements. So, in surge, simplified models for tower or blade (cases 1, 2 and 3) provide comparable results with those of rigorous FEM model (case 4). Fig. 4 compares heave motion. Four cases generally agree but the results are slightly different from rigorous model (case 4) when the lumped model is used for blade (case 1 and 3). The reason is that blade dynamics affects heave of floating body and lumped blade model does not calculate exact dynamics of blade. However, in a statistical sense, the variations of the four cases are similar (see Table 6 and 7 for comparing statistical average height of heave for each case). Fig. 5 compares pitch motion. Fig. 6 compares mooring line tensions. Tension of mooring line in connection part at bow fairlead is compared because the tension is the biggest in the line. Pitch and line tension are similar in four cases. Fig. 7 compares tower base stress of each case. Unlike other responses, tower base stress is significantly affected by dynamic elastic behavior of tower. Therefore, base stresses of simplified rigid tower model (case 1 and 2) are much different from the rigorous FEM model (case 4). Case 3 and 4 are very similar (see Fig. 7(d)) and it seems that elastic tower and lumped blade is a good choice in calculation of tower base stress. For more quantitative comparison, statistical responses of cases 1~3 are measured and the relative differences from case 4 are obtained. Statistical average heights are calculated by mean upcrossing method. The results are summarized in Table 6. Relative errors of cases 1~3 are all less than 5% except tower base stress. In tower bases stress, the error is bigger than 20% in simplified tower models. The effect of tower modeling on body motions and mooring line tensions looks small. On the other hand, tower base stress shows big difference by whether the tower model is a simplified one (cases 1 and 2) or elastic FEM one (cases 3 and 4). The reason is that tower base stress is directly affected by the modeling methods for tower and simplified models without elastic effect may give erroneous results. So, it could be said that tower modeling is more critical in coupled analysis of floating wind turbine. The results in higher waves (sea state 8) are also summarized in Figs. 8-12 and Table 7. The trends are similar to sea state 5.

Table 6 Comparison of statistical responses in sea state 5

Responses	Average height			
	Case 4	Case 1	Case 2	Case 3
Surge (m)	1.1625	1.2026 (3.45%)	1.1968 (2.95%)	1.1690 (0.56%)
Heave (m)	0.20380	0.20444 (0.31%)	0.20393 (0.07%)	0.20446 (0.32%)
Pitch (deg)	0.59918	0.62761 (4.74%)	0.62324 (4.02%)	0.60446 (0.88%)
Mooring line tension (N)	44,485	45,799 (2.95%)	45,530 (2.35%)	44,796 (0.70%)
Tower base stress (MPa)	35.154	43.160 (**22.77**%)	42.946 (**22.17**%)	34.595 (-1.59%)

( ) = relative error

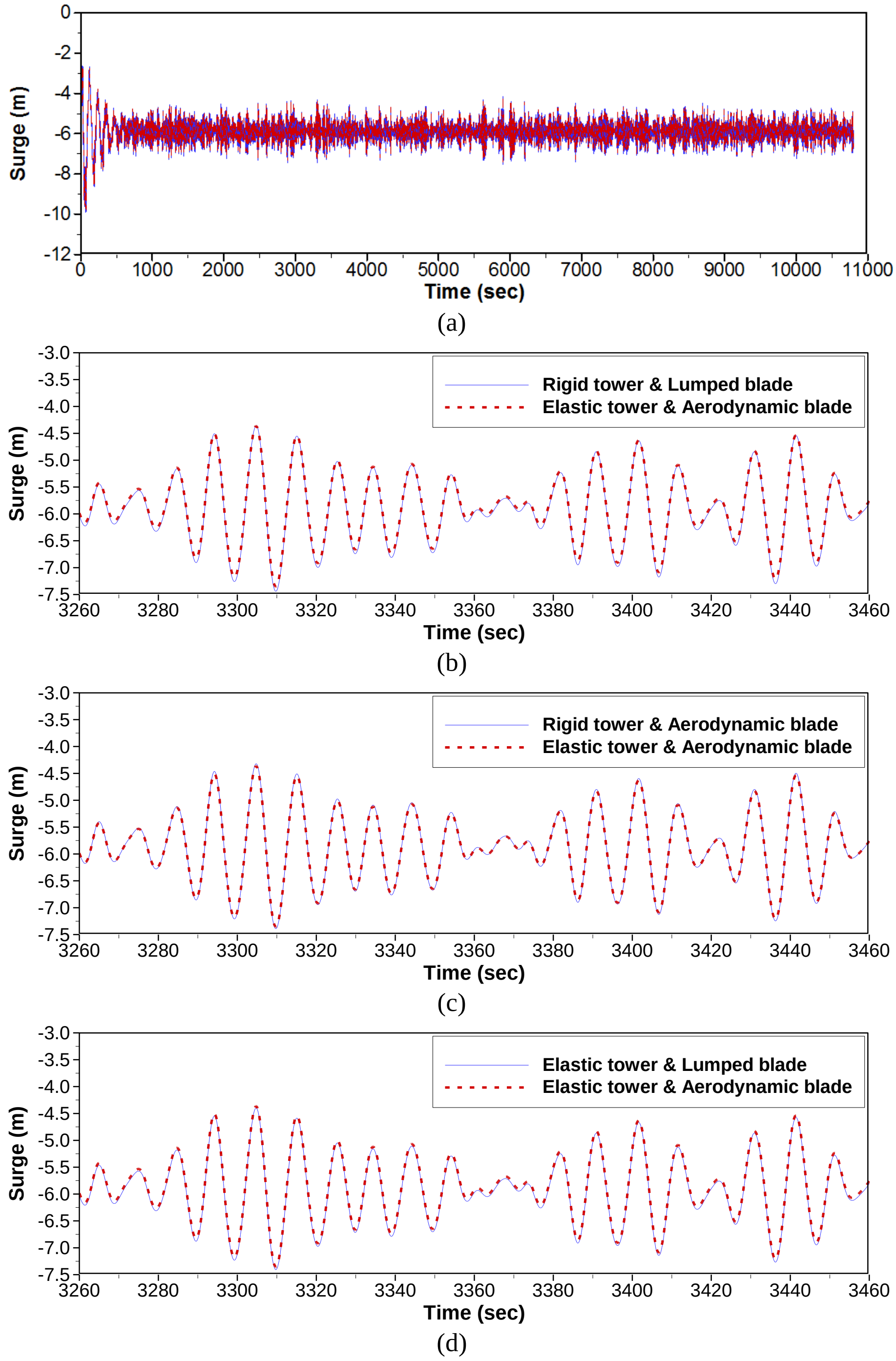

Fig. 3 (a) Comparison of surge in sea state 5 (full range), (b) Comparison of surge in sea state 5 (zoom range : case 1 vs 4), (c) Comparison of surge in sea state 5 (zoom range : case 2 vs 4) and (d) Comparison of surge in sea state 5 (zoom range : case 3 vs 4)

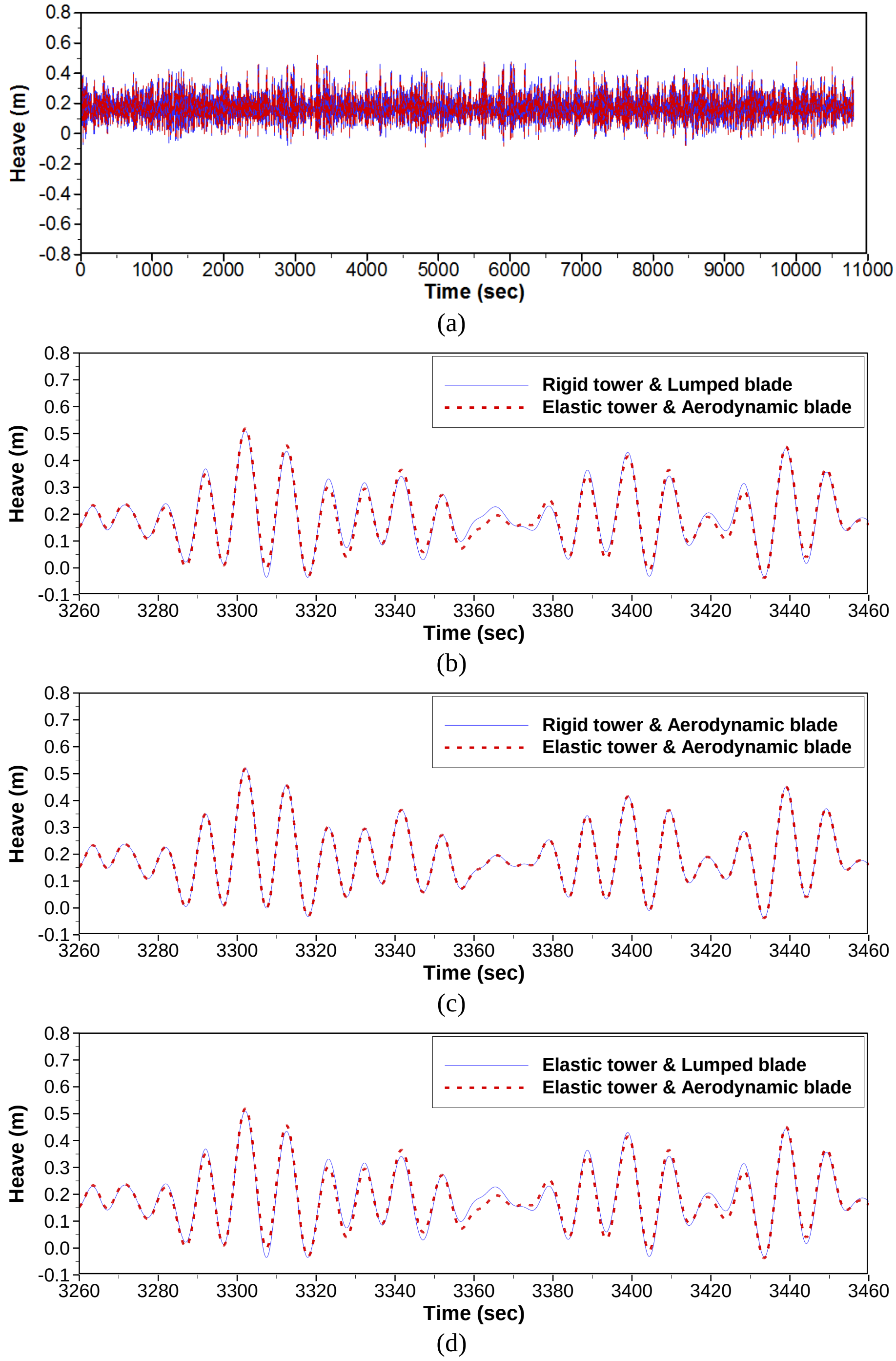

Fig. 4 (a) Comparison of heave in sea state 5 (full range), (b) Comparison of heave in sea state 5 (zoom range : case 1 vs 4), (c) Comparison of heave in sea state 5 (zoom range : case 2 vs 4) and (d) Comparison of heave in sea state 5 (zoom range : case 3 vs 4)

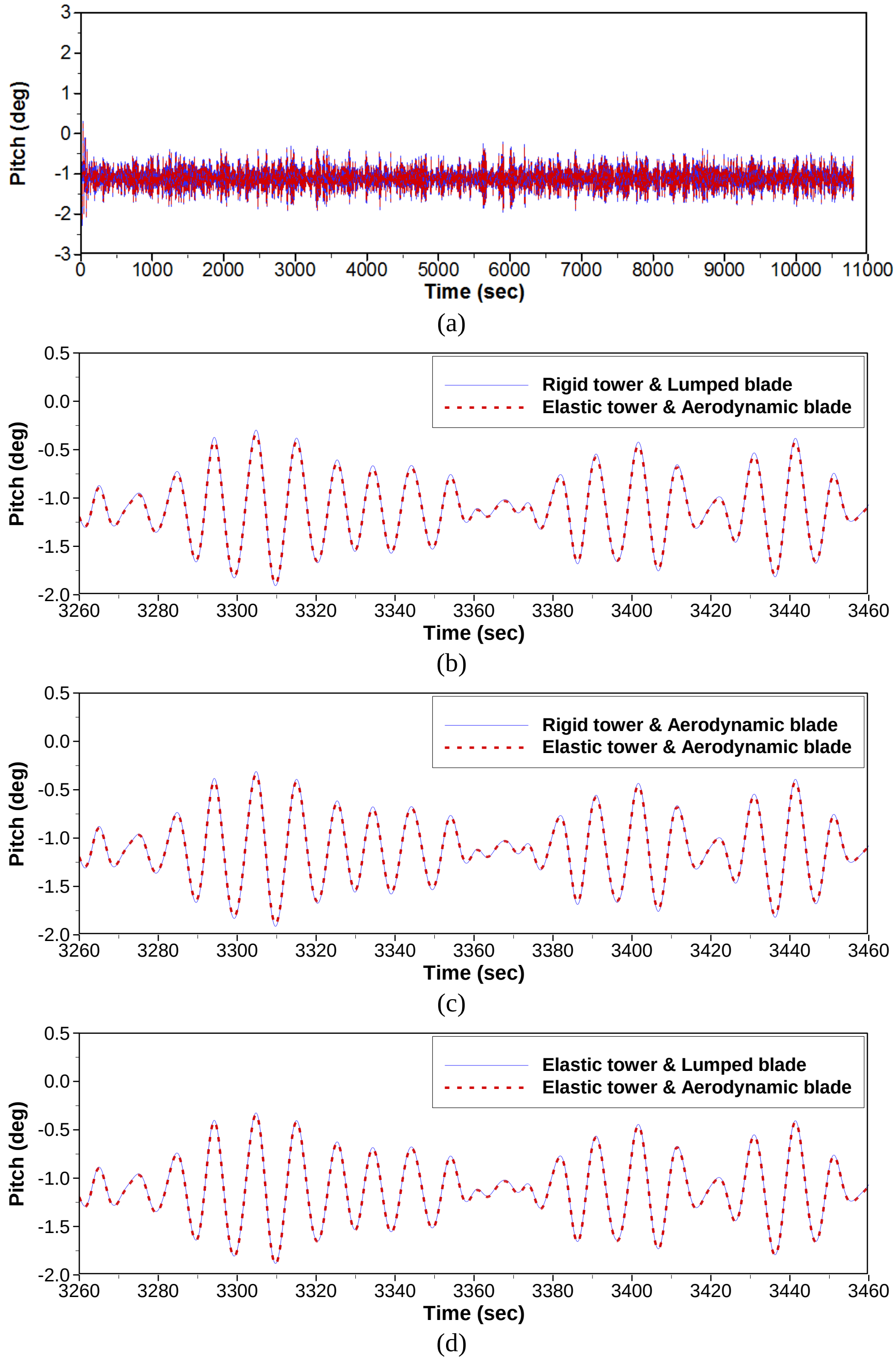

Fig. 5 (a) Comparison of pitch in sea state 5 (full range), (b) Comparison of pitch in sea state 5 (zoom range : case 1 vs 4), (c) Comparison of pitch in sea state 5 (zoom range : case 2 vs 4) and (d) Comparison of pitch in sea state 5 (zoom range : case 3 vs 4)

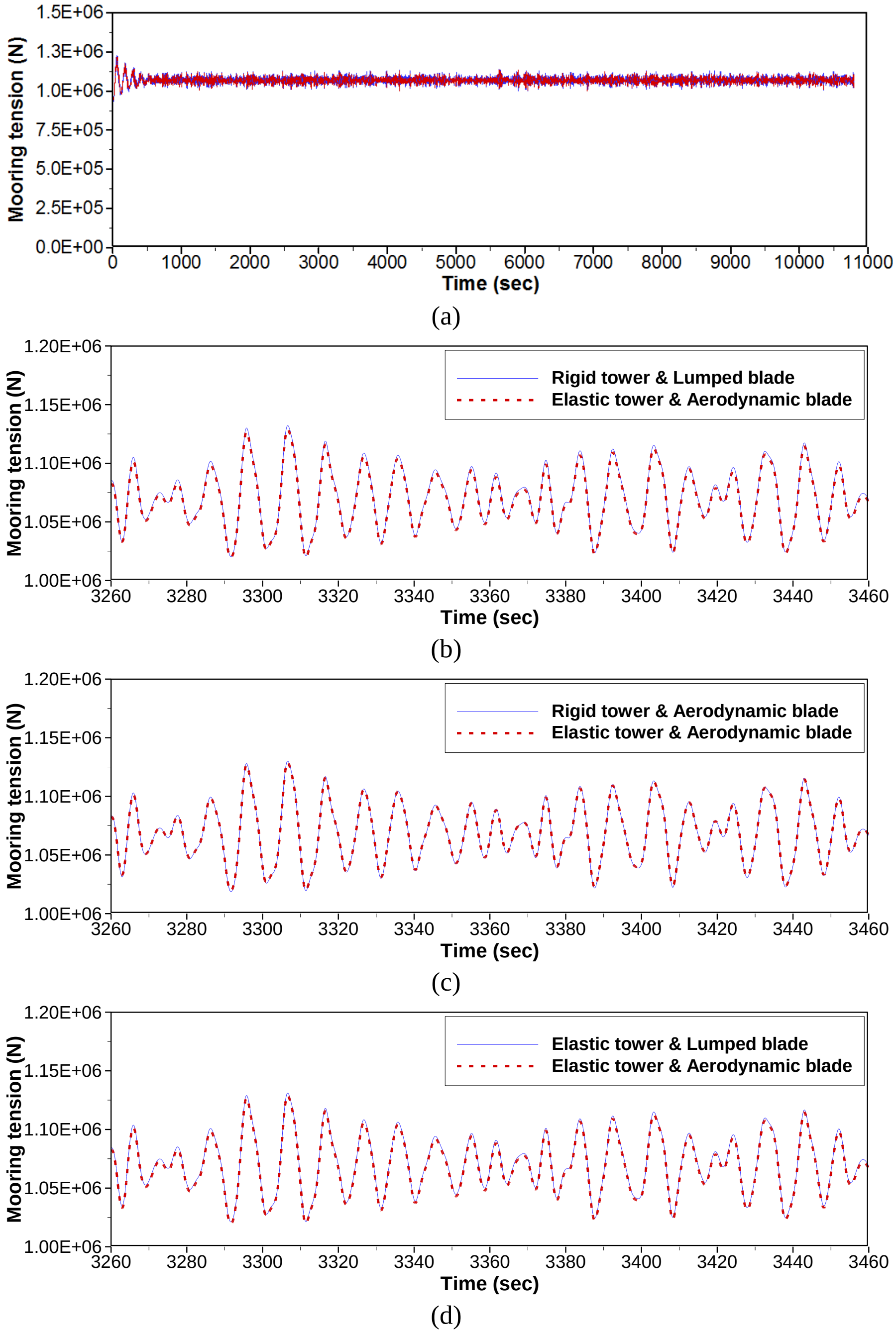

Fig. 6 (a) Comparison of mooring line tension in sea state 5 (full range), (b) Comparison of mooring line tension in sea state 5 (zoom range : case 1 vs 4), (c) Comparison of mooring line tension in sea state 5 (zoom range : case 2 vs 4) and (d) Comparison of mooring line tension in sea state 5 (zoom range : case 3 vs 4)

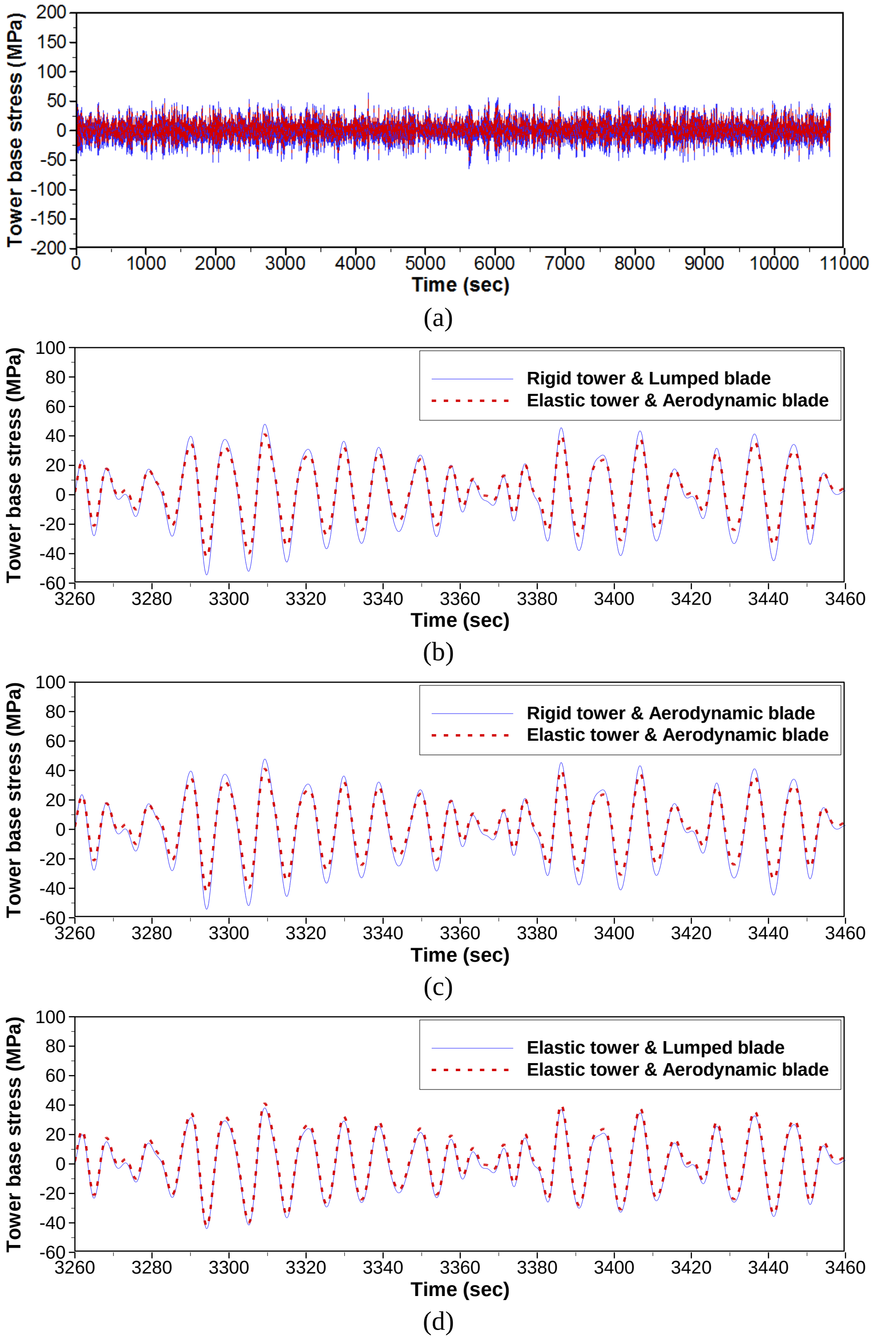

Fig. 7 (a) Comparison of tower base stress in sea state 5 (full range), (b) Comparison of tower base stress in sea state 5 (zoom range : case 1 vs 4), (c) Comparison of tower base stress in sea state 5 (zoom range : case 2 vs 4) and (d) Comparison of tower base stress in sea state 5 (zoom range : case 3 vs 4)

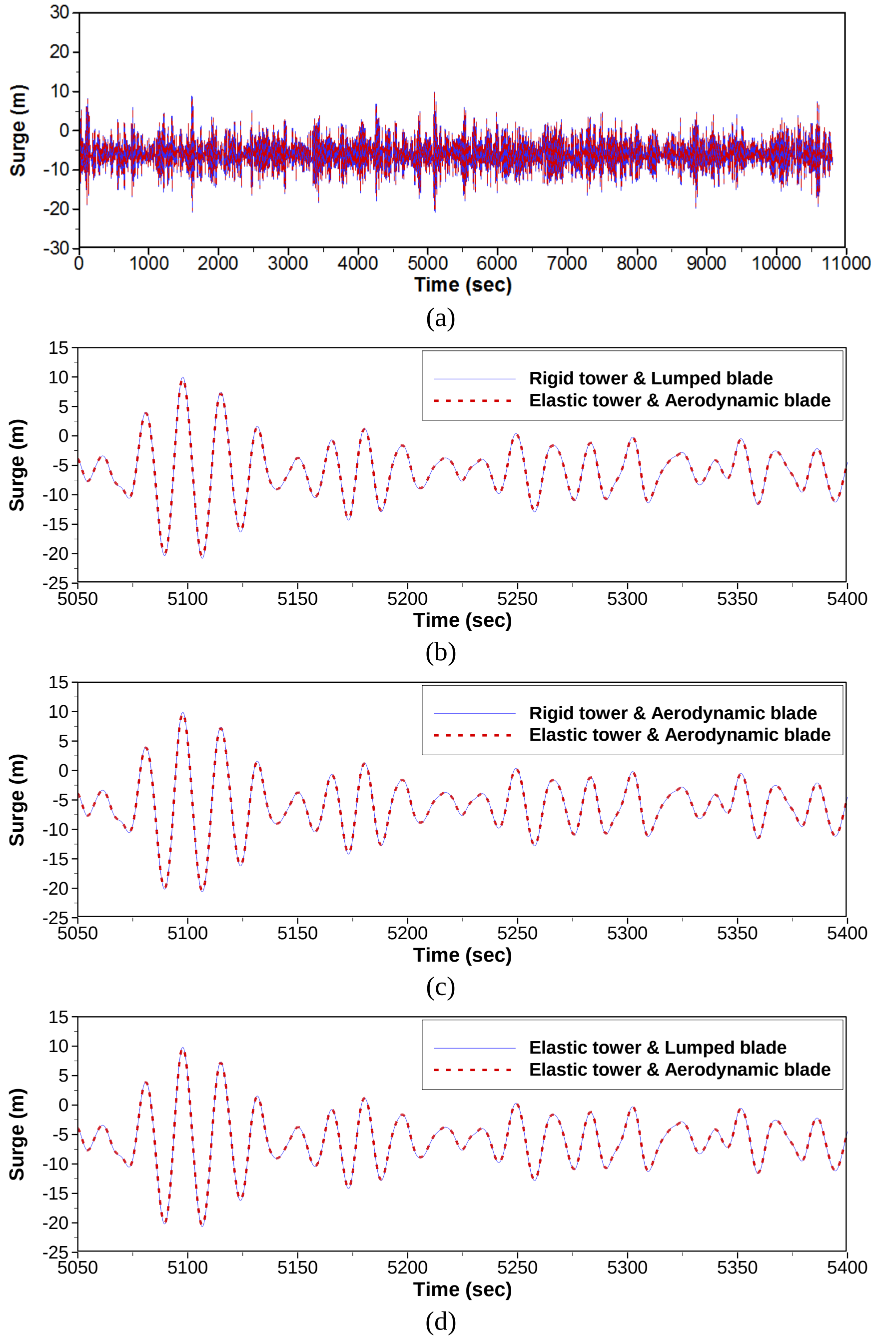

Fig. 8 (a) Comparison of surge in sea state 8 (full range), (b) Comparison of surge in sea state 8 (zoom range : case 1 vs 4), (c) Comparison of surge in sea state 8 (zoom range : case 2 vs 4), (d) Comparison of surge in sea state 8 (zoom range : case 3 vs 4)

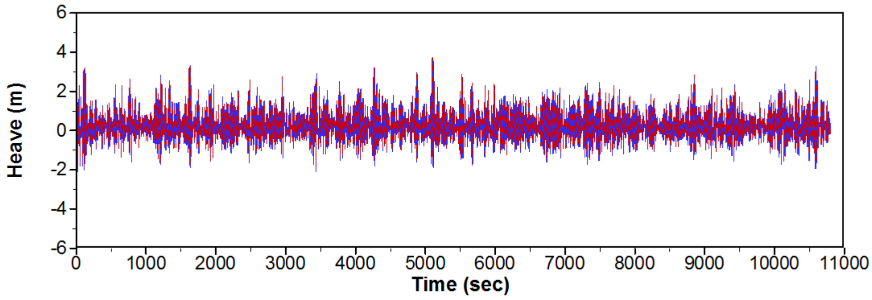

(a)

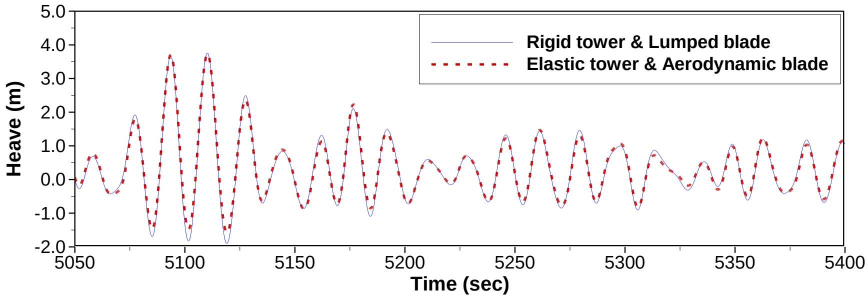

(b)

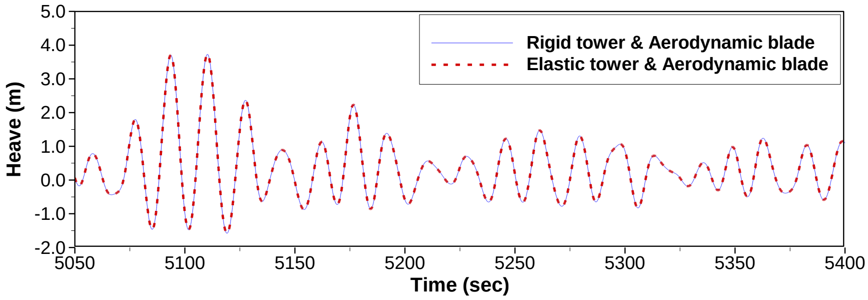

(c)

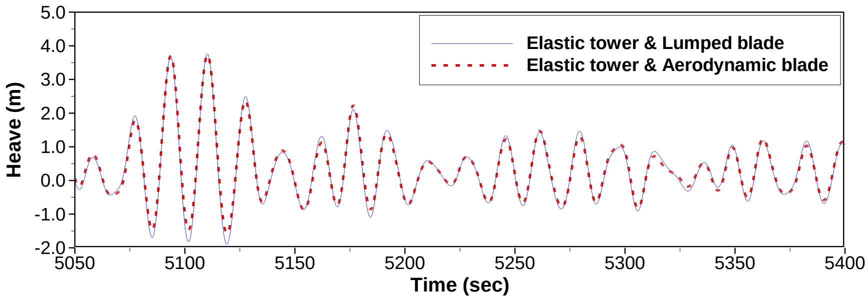

(d)

Fig. 9 (a) Comparison of heave in sea state 8 (full range), (b) Comparison of heave in sea state 8 (zoom range : case 1 vs 4), (c) Comparison of heave in sea state 8 (zoom range : case 2 vs 4) and (d) Comparison of heave in sea state 8 (zoom range : case 3 vs 4)

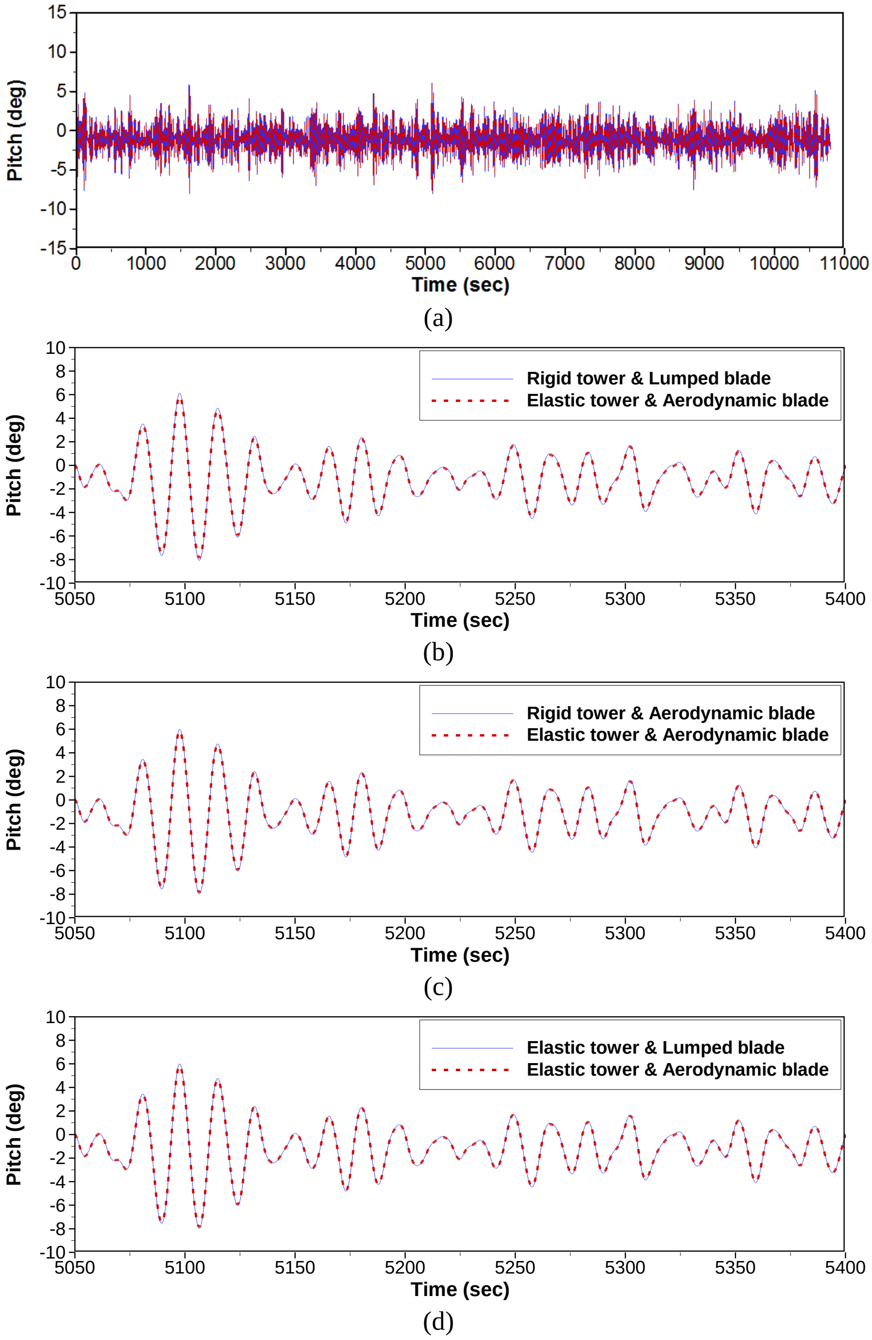

Fig. 10 (a) Comparison of pitch in sea state 8 (full range), (b) Comparison of pitch in sea state 8 (zoom range : case 1 vs 4), (c) Comparison of pitch in sea state 8 (zoom range : case 2 vs 4) and (d) Comparison of pitch in sea state 8 (zoom range : case 3 vs 4)

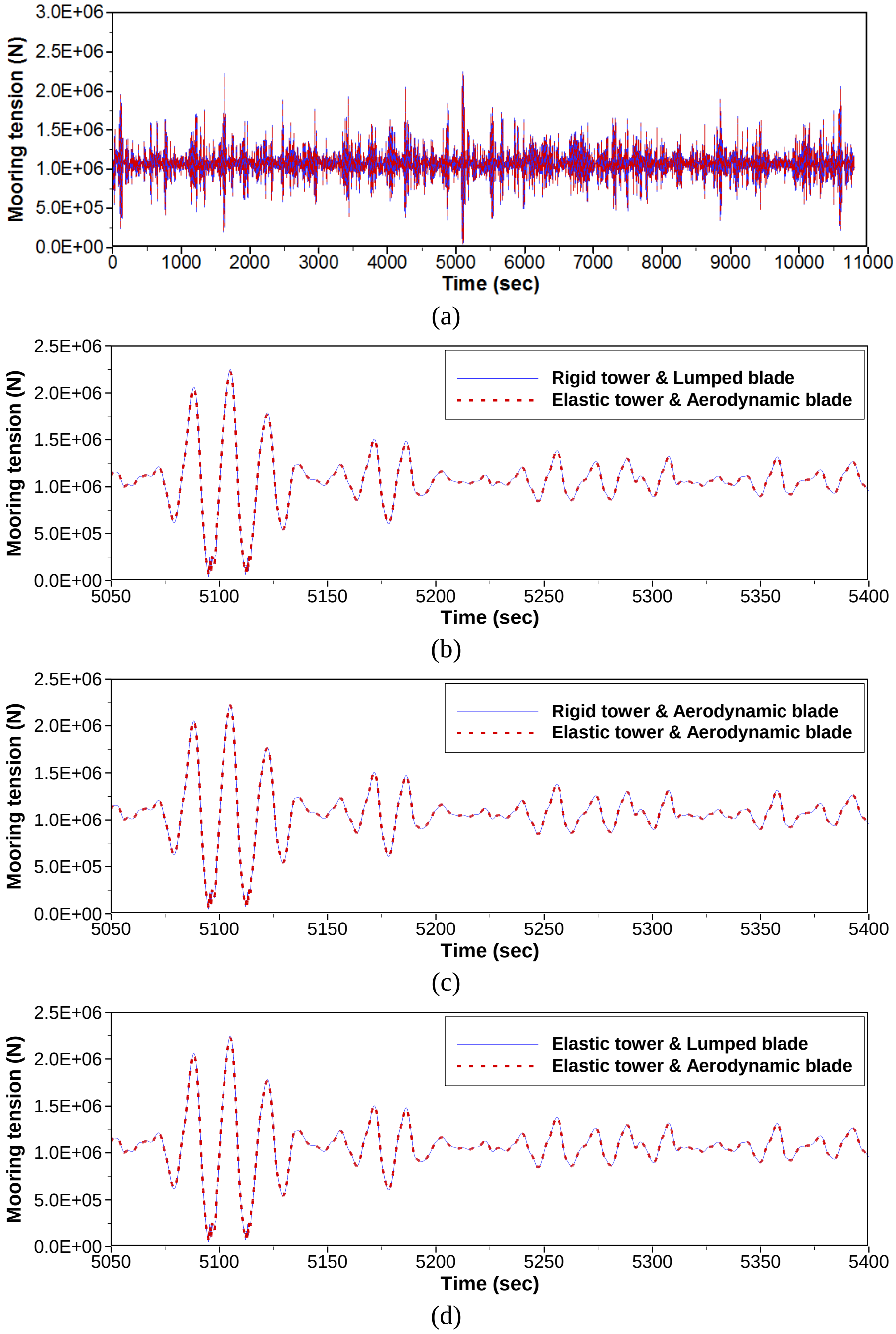

Fig. 11 (a) Comparison of mooring line tension in sea state 8 (full range), (b) Comparison of mooring line tension in sea state 8 (zoom range : case 1 vs 4), (c) Comparison of mooring line tension in sea state 8 (zoom range : case 2 vs 4) and (d) Comparison of mooring line tension in sea state 8 (zoom range : case 3 vs 4)

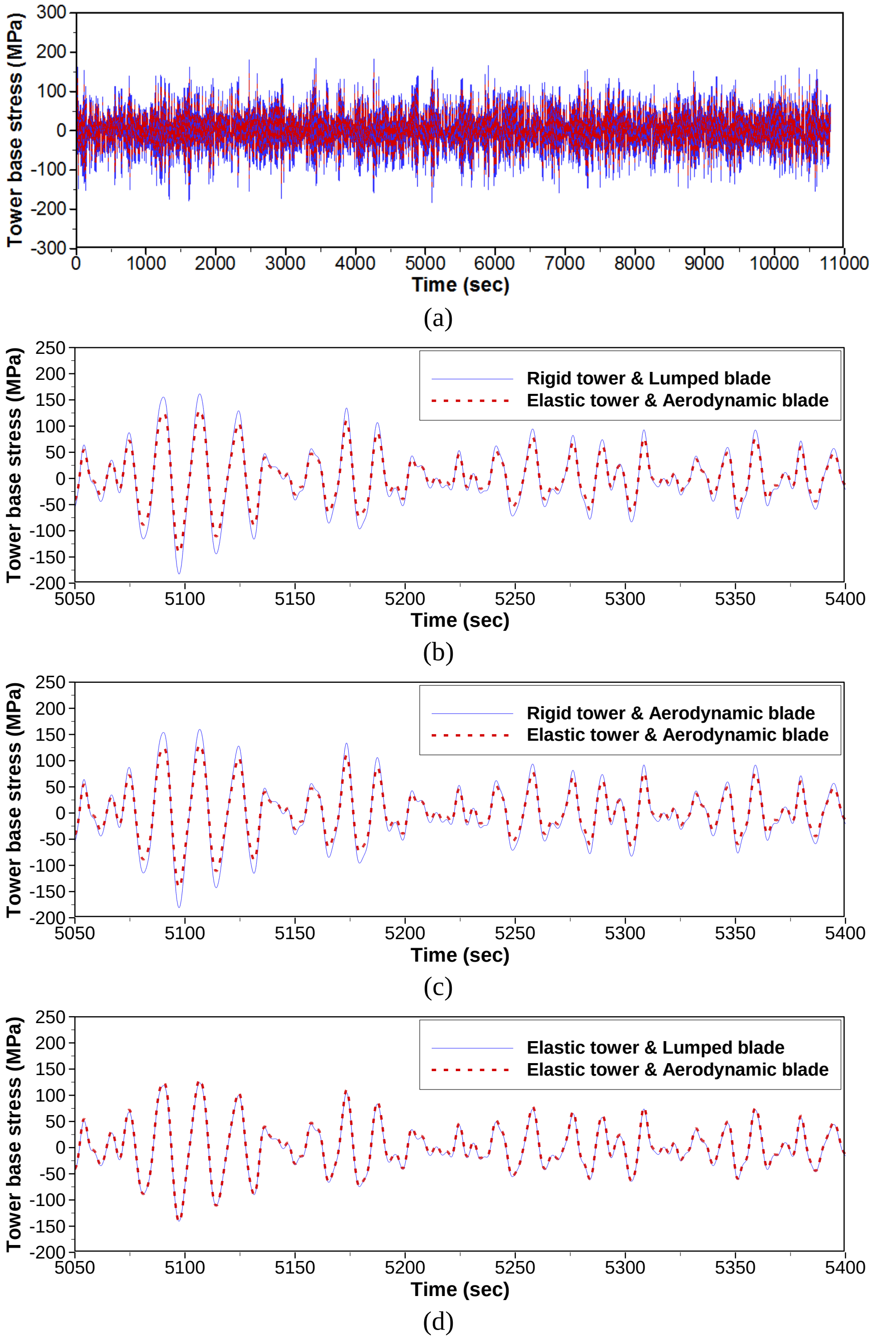

Fig. 12 (a) Comparison of tower base stress in sea state 8 (full range), (b) Comparison of tower base stress in sea state 8 (zoom range : case 1 vs 4), (c) Comparison of tower base stress in sea state 8 (zoom range : case 2 vs 4) and (d) Comparison of tower base stress in sea state 8 (zoom range : case 3 vs 4)

Table 7 Comparison of statistical responses in sea state 8

Responses	Average height			
	Case 4	Case 1	Case 2	Case 3
Surge (m)	9.2585	9.4301 (1.85%)	9.3722 (1.23%)	9.3602 (1.10%)
Heave (m)	1.8342	1.9153 (4.42%)	1.8341 (-0.01%)	1.9153 (4.43%)
Pitch (deg)	4.2580	4.4164 (3.72%)	4.3496 (2.15%)	4.3297 (1.68%)
Mooring line tension (N)	363,438	371,161 (2.12%)	364,869 (0.39%)	369,386 (1.64%)
Tower base stress (MPa)	100.30	126.04 (**25.67**%)	124.82 (**24.45**%)	97.888 (-2.40%)

( ) = relative error

4. Conclusions

This paper compares simplified rigid or lumped model and rigorous FEM model for tower and blade in dynamic coupled analysis of floating wind turbine. BEM with convolution and FEM with catenary were applied in formulating coupled equations for floating body and mooring lines, respectively. Elastic beam elements and elastic rotating aerodynamic beam elements were used in FEM model for tower and blade, respectively. A SPAR type moored wind turbine in wind and irregular waves is considered in numerical example. Surge, heave, pitch, mooring line tension and tower base stress with numerical models such as rigid tower & lumped blade, rigid tower & aerodynamic blade and elastic tower & lumped blade are analyzed and the results are compared with those of the rigorous model (elastic tower & aerodynamic blade). The conclusions are derived from numerical analyses results.

Rigid tower & lumped blade, rigid tower & aerodynamic blade and elastic tower & lumped blade show general agreements with elastic tower & aerodynamic blade in surge, heave, pitch and mooring line tensions. However, tower base stresses of rigid tower & lumped blade and rigid tower & aerodynamic blade are much different those of elastic tower & aerodynamic blade. On the other hand, tower base stresses of elastic tower & lumped blade and elastic tower & aerodynamic blade are similar. Therefore, modeling of tower looks more critical in coupled analysis of floating wind turbine structure.

Acknowledgements

This research is a part of "Pre-FEED Poject" by Korea Ministry of Oceans and Fisheries and "Basic R&D Program" by KRISO.

References

Bae, Y.H., Kim, M.H., Im, S.W. and Chang, I.H. (2011), "Aero-elastic-control-floater-mooring coupled dynamic analysis of floating offshore wind turbines", *ISOPE 2011*, 429-435.

Bae, Y.H., Kim, M.H. and Im, S.W. (2012), "Effects of tower elasticity and aero-loading in aero-elastic-control-floater-mooring coupled dynamic analysis for a TLP-type FOWT", *ISOPE 2012*, 324-329.

Bae, Y.H., Kim, M.H. and Yu, Q. (2013), "Coupled dynamic analysis of FOWT (Floating Offshore Wind Turbine) with partially broken blade", *ISOPE 2013*, 352-358.

Bae, Y.H., Kim, M.H. and Yu, Q. (2014), "The dynamic coupling effects of a MUFOWT (Multiple Unit Floating Offshore Wind Turbine) with partially broken blade", *ISOPE 2014*, 317-324.

Choi, Y.R., Hong, S.Y. and Choi, H.S. (2000), "An analysis of second-order wave forces on floating bodies by using a higher-order boundary element method", *Ocean Eng.*, **28**, 117-138.

Chung, J. and Hulbert, G.M. (1993), "A time integration algorithm for structural dynamics with improved numerical dissipation : The generalized α-method", *J. Appl. Mech. -T ASME*, **60**, 371-375.

Cummins, W.E. (1962), "The impulse response function and ship motions", *Symposium on Ship Theory at the Institut fur Schiffbau der Universitat Hamburg*.

Garrett, D.L. (2005), "Coupled analysis of floating production systems", *Ocean Eng.*, **32**, 802-816.

Hamming, R.W. (1959), "Stable predictor-correct methods for ordinary differential equations", *J. ACM*, **6**, 37-47.

Hong, S. and Hong, S.Y. (1997), "Effects of mooring line dynamics on position keeping of a floating production system", *ISOPE 1997*, 336-341.

Hong, S.Y., Kim, J.H., Cho, S.K., Choi, Y.R. and Kim, Y.S. (2005), "Numerical and experimental study on hydrodynamic interaction of side-by-side moored multiple vessels", *Ocean Eng.*, **32**(7), 783-801.

Jonkman, J. (2010), *Definition of the floating system for phase IV of OC3*, NREL/TP-500-47535.

Jonkman, J., Butterfield, S., Musial, W. and Scott, G. (2009), *Definition of a 5-MW reference wind turbine for offshore system development*, NREL/TP-500-38060.

Jonkman, J. and Musial, W. (2010), *Offshore code comparison collaboration (OC3) for IEA task 23 offshore wind technology and deployment*, NREL/TP-5000-48191.

Kim, B.W., Sung, H.G., Hong, S.Y. and Jung, H.J. (2010), "Finite element nonlinear analysis for catenary structure considering elastic deformation", *Comput. Model. Eng. Sci.*, **63**, 29-45.

Kim, B.W., Sung, H.G., Kim, J.H. and Hong, S.Y. (2013), "Comparison of linear spring and nonlinear FEM methods in dynamic coupled analysis of floating structure and mooring system", *J. Fluids Struct.*, **42**, 205-227.

Kim, M.H., Ran, Z., Zheng, W., Bhat, S. and Beynet, P. (1999), "Hull/Mooring coupled dynamic analysis of a truss spar in time-domain", *ISOPE 1999*, 301-308.

Shim, S. and Kim, M.H. (2008), "Rotor-floater-tether coupled dynamic analysis of offshore floating wind turbines", *ISOPE 2008*, 455-460.